Crystallization Behavior of Poly(ethylene terephthalate) Blended with Hyperbranched Polymers: The Effect of Terminal Groups and Composition of Hyperbranched Polymers

Jyongsik Jang,*,† Joon Hak Oh,† and Sung In Moon‡

School of Chemical Engineering, College of Engineering, Seoul National University, Shinlimdong San 56-1, Seoul, Korea, and Saehan Industries Inc., Yongin City, Kyunggi-Do, Korea

Received September 20, 1999; Revised Manuscript Received December 13, 1999

ABSTRACT: The effects of terminal groups and composition of hyperbranched polymers (HBPs) on the crystallization behavior of poly(ethylene terephthalate) (PET) in HBP/PET blends were investigated using in situ FT-IR spectroscopy and differential scanning calorimetry. Hyperbranched aliphatic polyester was synthesized from an AB_2 type monomer and a B_3 type core. The hydroxyl terminal groups of the HBP were transformed into acetate and benzoate groups by organic synthetic methods. The effects of the HBPs were compared with those of linear polyester (LPE) synthesized from an AB type monomer and a B_2 type core. A small amount of HBP with hydroxyl groups could greatly reduce the relative crystallinity of PET through hydrogen bonds. HBP with acetate groups showed effects similar to those of LPE. As the composition of LPE was increased, the relative crystallinity of PET was slightly decreased. On the contrary, HBP with benzoate groups played the role of nucleating agent in the blends with PET. The crystallization rate of PET was highest in the blend with 12 wt % HBP. Dynamic viscosity measurements were performed to investigate the role of the HBPs as processing aids.

Introduction

Hyperbranched polymers (HBPs) and dendrimers have attracted considerable and increasing interest during recent years.[1−4] Dendrimers consist of AB_x type ($x \geq 2$) monomers attached in layers around a central core, where each layer is called a generation. They have perfectly branched structures. HBPs resemble dendrimers with the difference that they have randomly branched structures and contain varying amounts of linear segments. Compared with dendrimers obtained from multistep syntheses,[5,6] HBPs are more advantageous as they can be easily synthesized through one-step polymerization processes.[7,8] Because of their highly functionalized globular structures, HBPs exhibit different properties from those of linear polymers of the same molar mass, such as less entanglement in the solid state,[9] high solubility in various solvents, and low melt viscosity.[10−12] Terminal groups of HBPs have a great influence on their physical properties such as glass transition temperature (T_g),[13] relaxation process,[14] viscosity,[15] and solubility.[16]

Although there has been much progress in the structural understanding and the methods of synthesis of HBPs, applications of HBPs to practical situations have rarely been carried out. Boogh et al.[17] reported that HBPs exhibited outstanding performance as tougheners in epoxy resins. Gopala et al.[18] utilized hyperbranched polyester as a rheological modifier and toughening agent in bismaleimide. Despite high potential for good performance, the blends of HBPs with other linear polymers have rarely been studied. Novel blends of HBPs with linear polymers were studied by Massa et al.[19] The study was focused on the miscibility of blends. It has been reported that the addition of small perfect dendritic polyesters to poly(ethylene terephthalate) (PET) can yield miscible blends.[20] However, these studies did not give any information concerning the effects of dendritic materials on the crystallization behaviors of semicrystalline polymers. During the manufacturing process of semicrystalline polymers, controlling the crystallization rate is of great importance to obtain the products with desired properties. In addition, melt viscosity is an important factor in determining the processing temperature.

Therefore, it is the purpose of this study to investigate the effects of HBPs on the crystallization behavior of semicrystalline polymers and to study the role of HBPs as processing aids in their blends. Experimental parameters were the terminal groups and the composition of HBPs. Hyperbranched aliphatic polyester, which was synthesized from an AB_2 type monomer and a B_3 type core, was used. PET was chosen as the semicrystalline polymer because it has been used in a large amount of industrial applications. The effects of HBPs were compared with those of a linear analogue synthesized from an AB type monomer and a B_2 type core, where the branching was perfectly suppressed and the backbone was very similar to those of the HBPs. Crystallization behaviors were investigated by in situ FT-IR spectroscopy and differential scanning calorimetry (DSC). Melt viscosity measurements were performed using a rheometer to investigate the viscosity drop in the blend systems. The synergic effects of this blend system were considered to be the lowering of the processing temperature of PET, the suppression of the fast crystallization of PET, the softening and toughening of PET films, and the enhancement of solvent resistance of HBP.

Experimental Section

Materials. 2,2-Bis(methylol)propionic acid (bis-MPA) was used as an AB_2 type monomer, and 2-ethyl-2-(hydroxymethyl)-1,3-propanediol (trimethylolpropane: TMP) was used as a B_3 type core moiety. *p*-Toluenesulfonic acid (*p*-TSA) was used as an acid catalyst. Acethyl chloride, benzoyl chloride, 4-(dimethylamino)pyridine (DMAP), and triethylamine (TEA) were used to change the terminal groups of the HBP. All of these chemicals were purchased from Aldrich and used without

† Seoul National University.
‡ Saehan Industries Inc.
* To whom correspondence should be addressed. Tel 82-2-880-7069; Fax 82-2-888-1604; E-mail jsjang@plaza.snu.ac.kr.

10.1021/ma991592c CCC: $19.00
Published on Web 02/17/2000

Scheme 1. Schematic Diagram for the Transformation of the Terminal Groups of HBP(OH)

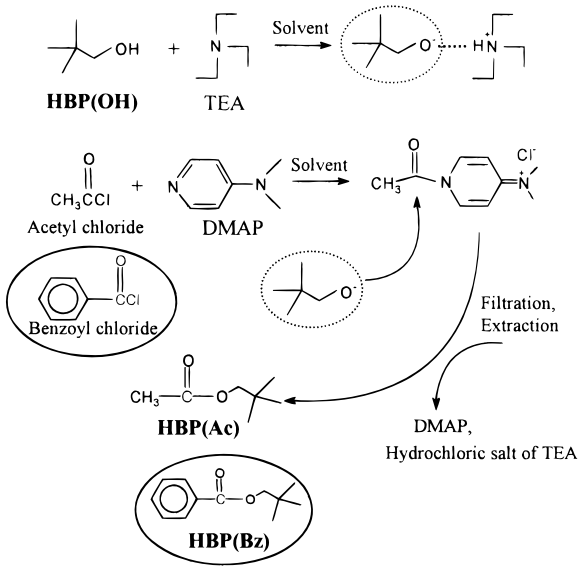

further purification. Hydroxypivalic acid (AB type monomer) and 2-ethyl-2-methyl-1,3-propanediol (B_2 type core) were purchased from Tokyo Chemical Industry Co. (Japan) and used to synthesize the linear analogue of the HBP. PET (M_v = ca. 18 000 g/mol, T_g = 81 °C) was provided by Samyang Co. (Korea).

Sample Preparation. Synthesis of HBPs. Bis-MPA (149 mmol, 20.0 g), TMP (7.1 mmol, 0.953 g) (in stoichiometric correspondence to the perfect third generation, i.e., bis-MPA: TMP = 21:1), and *p*-TSA (0.100 g) were well mixed in a three-necked flask equipped with a nitrogen inlet, a drying tube, and a mechanical stirrer. The flask was placed in an oil bath previously heated to 140 °C, and the mixture was left to react for 3 h under stirring. The nitrogen stream was turned off, and the flask was connected to a vacuum line for 2 h. The molecular weight of the synthesized HBP was evaluated using a matrix-assisted laser desorption−ionization time-of-flight (MALDI/TOF) mass spectrometer, i.e., M_n = 1688 g/mol. The hydroxyl terminal groups of the HBP were transformed into acetate (Ac) and benzoate groups (Bz) using TEA and DMAP as catalysts.[14] The procedure for the change of the terminal groups of the HBP is schematically outlined in Scheme 1.

Synthesis of Linear Polyester (LPE). Hydroxypivalic acid (80.9 mmol, 9.556 g), 2-ethyl-2-methyl-1,3-propanediol (3.85 mmol, 0.455 g), and *p*-TSA (48 mg) were well mixed in a three-necked flask equipped with a nitrogen inlet, a drying tube, and a mechanical stirrer. The flask was moved to an oil bath at 130 °C. The mixture was left to react for 2 h under nitrogen atmosphere. Subsequently, the flask was connected to a vacuum line for 2 h. The molecular weight of LPE was also evaluated using a MALDI/TOF mass spectrometer, i.e., M_n = 1445 g/mol.

Solution Blends. HBP/PET blends were prepared by the solution precipitation method. The compositions of HBP/PET blends were 4/96, 12/88, and 20/80 by wt %. Small ratios of the HBPs to PET were chosen because the small quantity of the HBPs could show sufficient interaction with PET due to their multifunctionality. The HBPs and PET were dissolved in 100 mL of 1,1,2,2-tetrachloroethane (TCE)/phenol (40/60 by vol %) cosolvent, and the solution mixture was precipitated in the 20-fold excess volume of methanol. The coprecipitant was filtered, washed several times with hot methanol to remove residual phenol, and dried in a vacuum oven at 100 °C for a day. Several drops of the blend solution were coated onto a KBr pellet with a spoid, and the pellet was dried in a vacuum oven at 100 °C for 2 h. Then, the pellet was covered with another pure KBr pellet and set up on in situ FT-IR spectroscopic apparatus for isothermal crystallization analysis.

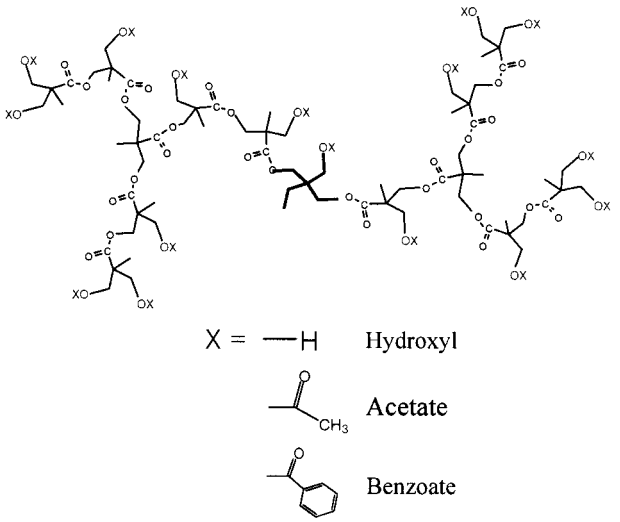

Figure 1. Chemical structures of HBP and transformed end groups.

Instrumental Analysis. Infrared spectra were recorded on a Bomem MB 100 Fourier transform infrared (FT-IR) spectrometer equipped with a deuterated triglycine sulfate (DTGS) detector. In situ FT-IR analysis was performed in a heating block equipped with a temperature controller. IR spectra were obtained in the absorption mode at a resolution of 2 cm^{-1} and 16 coaddition. The sample in the in situ FT-IR spectroscopic apparatus was heated to 275 °C at the heating rate of 20 °C/min and held for 5 min in order to remove the thermal history. Then, it was cooled to the isothermal crystallization temperature (T_c), 210 °C. The T_c was chosen as a value slightly higher than the melt crystallization temperature (T_{mc}) in order to suppress the fast crystallization of PET during the cooling or quenching processes to T_c. DSC analysis was performed on a Perkin-Elmer DSC-7. In the isothermal experiment, the sample was heated to 275 °C at a heating rate of 20 °C/min, kept for 5 min, and quenched to T_c at a cooling rate of 200 °C/min. The corresponding crystallization exotherm was obtained as a function of time until no change was observed. In the dynamic experiment, the sample was heated to 275 °C, kept for 5 min, and cooled to 150 °C at a cooling rate of 10 °C/min. MALDI/TOF mass spectra were recorded on a Voyager Biospectrometry workstation mass spectrometer (PerSeptive Biosystems Inc., Framingham, MA: laser pulse width = 3 ns, laser wavelength = 337 nm). The experimental mode was a positive mode. The accelerating voltage was fixed at 20 kV, the grid voltage 80%, and the guide wire voltage 0.1%. The matrix solution was prepared as dithranol/tetrahydrofuran (10 mg/1 mL). Rheological measurements were performed with a RMS-800 (Rheometrics Co.). The experimental mode was a dynamic frequency sweep test using a parallel plate geometry. The strain constant was fixed at 2%. The frequency range was 0.1−10 rad/s, and the experimental temperature was 270 °C.

Results and Discussion

We have recently reported the synthetic process and the microstructure of hyperbranched aliphatic polyester used in this study using in situ FT-IR spectroscopy, ^{13}C NMR, and MALDI/TOF mass spectroscopy.[21] The chemical structures of the HBP and the transformed end groups are illustrated in Figure 1. The degree of branching (DB) of the HBP was determined to be 0.44 by the inverse gated decoupling ^{13}C NMR technique.

Figure 2 represents FT-IR spectral difference due to the transformation of the terminal groups of HBP. The principal vibrational bands of HBPs and their assignments are listed in Table 1. The stretching band of hydroxyl groups near 3500 cm^{-1} disappeared from the FT-IR spectra of the HBPs with acetate (HBP(Ac)) and

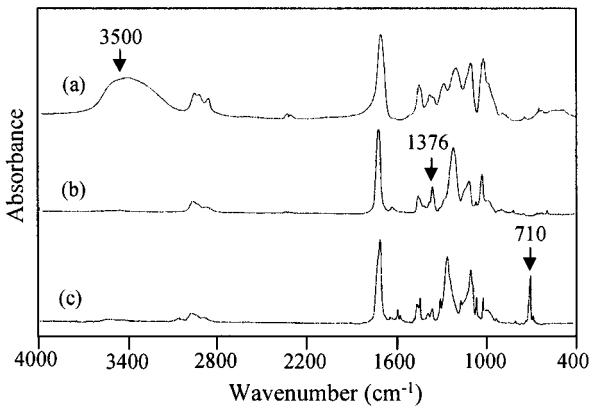

Figure 2. FT-IR spectra of HBPs with different end groups: (a) HBP(OH), (b) HBP(Ac), and (c) HBP(Bz).

benzoate groups (HBP(Bz)). In the spectrum of HBP(Ac), the peak at 1376 cm^{-1} was due to the CH_3 bending vibration, which was enhanced by an adjacent carbonyl group and characteristic of acetates. In the case of HBP(Bz), the band at 710 cm^{-1} was assigned to the ring C−H wagging vibration, which was characteristic of the benzene ring. Therefore, it is believed that the transformation of the terminal groups was successfully performed.

Figure 3 shows the carbonyl peak shift of pure PET on annealing at 210 °C. The C═O stretching band for PET with increasing crystallinity was shifted to lower wavenumbers. Since the number of hydroxyl groups required to form hydrogen bonds is much smaller than that of C═O groups, it is obvious that the effect of hydrogen bond on the C═O peak shift is not significant. This band shift is rather attributed to the difference in coplanarity of the C═O group with respect to the benzene ring. As the crystallinity of PET increases, the coplanarity between the ester group and the benzene ring increases due to the crystalline structure of PET. As the coplanar conformation with the benzene ring is enhanced, the conjugation of the ester group becomes stronger, resulting in a lower shift of the C═O peak. Therefore, the width of the band shift is proportional to the enhanced coplanarity and crystallinity.[22−24] The increase of dipole−dipole interaction with increasing crystallinity can also be a cause for the C═O peak shift. Other annealing sensitive peaks of PET are shown in Figure 4. The bands at 1369 (gauche CH_2 wag), 1099 (gauche C−O str (B type)), and 1042 cm^{-1} (gauche C−O str (A type)) became weaker in peak intensity with increasing the annealing time. On the contrary, the bands at 1343 (trans CH_2 wag) and 1118 cm^{-1} (trans CH_2 twist) became more intense. Those variations of the band intensities are associated with the change in molecular conformation of the ethylene glycol residue of PET with increasing annealing time, i.e., from gauche form to trans form.[25,26] In HBP/PET blends, all HBPs have carbonyl groups in their backbones. Moreover, HBP(Ac) and HBP(Bz) have carbonyl groups in their terminal groups. Therefore, it is difficult to surmise crystallinity from the C═O stretching peaks in these blend systems. Relative crystallinity can be defined from the integration of the peaks at 1343 and 1369 cm^{-1} as follows:

$$X(t) = \left(\frac{A_T}{A_T + A_G}\right) \times 100$$

where $X(t)$ is the relative crystallinity at time t, and A_T and A_G are the areas of the peaks due to trans and gauche CH_2 wagging vibrations, respectively. Since these two peaks were generated from the same molecular architecture and the sample amount was unchanged, correction by an internal reference peak was not needed.

Crystallization Behaviors of HBP/PET Blends. Table 2 exhibits the glass transition temperatures (T_g's) of HBPs and their blends. Single T_g's indicate that the blends were miscible. The T_g of the HBP(OH)/PET blend was higher than that expected from the Fox equation. This is thought to be from polar interaction, i.e., hydrogen bonds between the hydroxyl groups of HBP(OH) and the carbonyl groups of PET. The samples of HBP(OH)/PET blends were annealed in the in situ FT-IR spectroscopic apparatus at 210 °C for 1 h. The change in relative crystallinity with increasing annealing time is presented in Figure 5. As the composition of HBP(OH) was increased, the relative crystallinity of PET was greatly reduced. The decreasing slope of the tangent indicates that the crystallization rate of PET was also reduced.

Figure 6 shows the carbonyl peaks of the HBP(OH)/PET blends after 1 h annealing. In the case of HBP(OH)/PET blends, the red shift of C═O peaks could arise from the enhanced coplanarity and the increased dipole−dipole interaction, as well as from hydrogen bonds. In the blend with 4 wt % HBP(OH), HBP(OH) could not greatly affect the crystallinity on account of the small number of hydroxyl groups. Therefore, the red shift of the C═O band mainly arose from the enhanced coplanarity and the increased dipole−dipole interaction. In the early stage of annealing, the wavenumbers of C═O peaks in the blends with 12 and 20 wt % HBP(OH) were somewhat lower than that in the blend with 4 wt % HBP(OH). In the blends with 12 and 20 wt % HBP(OH), the amounts of hydroxyl groups were large enough to influence the crystallinity greatly. As the annealing time was increased, the crystallization of PET in the blends with 12 and 20 wt % HBP(OH) was greatly suppressed owing to the hydrogen bonds, whereas the crystallization of PET in the blend with 4 wt % HBP(OH) was less suppressed. Consequently, the C═O shift width in the blend with 4 wt % HBP(OH) was relatively larger than those in the blends with 12 and 20 wt % HBP(OH). In the case of the blends with 12 and 20 wt % HBP(OH), as the composition of HBP(OH) was increased the half-width of the C═O peaks was increased. The red shift of the C═O peaks with increasing the composition of HBP(OH) originated from the increment of hydrogen bonds formed between the hydroxyl terminal groups of HBP(OH) and the C═O groups of PET. The hydrogen bonds might inhibit PET from being aligned as the trans form and reduce the relative crystallinity of PET. The blue shift of the C═O peaks was derived from the weakening of dipole−dipole interaction and the reduction of coplanarity due to the reduced crystallinity. Since HBP(OH) had free C═O groups in its backbone, the increase of the composition of HBP(OH) induced the increase of free C═O groups. This could also broaden the half-width of C═O peak and lessen the shift width.

A small amount of HBP(OH) could largely reduce the crystallinity of PET. Considering that a large amount of linear amorphous polymers is required to significantly suppress the crystallization of PET,[22,27,28] HBP(OH) is much more useful for reducing the crystallinity of PET.

Table 1. Principal Vibrational Bands of HBPs and Their Assignments

HBP(OH)		HBP(Ac)		HBP(Bz)	
ν (cm^{-1})	assignment	ν (cm^{-1})	assignment	ν (cm^{-1})	assignment
3500 (s, b)[a]	OH str	1739 (vs)	C═O str (acetate)	2000−1800 (w)	summation bands
1730 (vs)	C═O str	1472 (m)	CH_3, CH_2 bend	1725 (vs)	C═O str (benzoate)
1475 (m)	CH_2 scissors def	1376 (s)	CH_3 umbrella bend	1602 (m), 1585 (m)	sym ring str
1456 (m)	CH_3 asym def	1238 (vs)	O−C(═O)−C str		
1390 (m)	CH_3 sym def	1044 (s + sh)	ester C−O str coupled to C−C	1491 (w)	different ring str
1220 (s)	C−C−O asym str			1472 (m), 1452 (m)	"sideways" ring bend + CH_3 asym bend
1037 (vs)	1° alcohol C−O str				
863 (m + sh)	CH_3 rock mixed with C−C str			1374 (m)	CH_3 sym bend
639 (m, b)	1° alcohol C−OH def			1270 (s)	benzoate ester C−O str
569 (w)	1° alcohol C−C−O bend			1112 (s)	OCH_2 str
				1071 (m), 1027 (m)	ring C−H bend
				710 (s)	ring C−H wag

[a] Intensity: s, strong; m, medium; w, weak; v, very; sh, shoulder; b, broad.

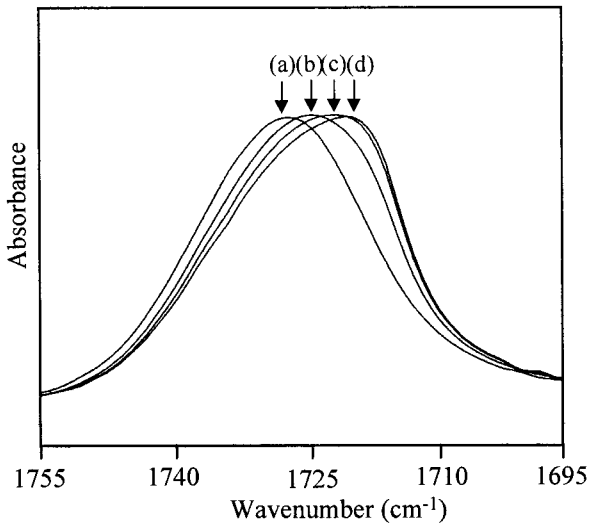

Figure 3. Carbonyl peak shift of PET on annealing at 210 °C: (a) 0, (b) 10, (c) 20, and (d) 60 min.

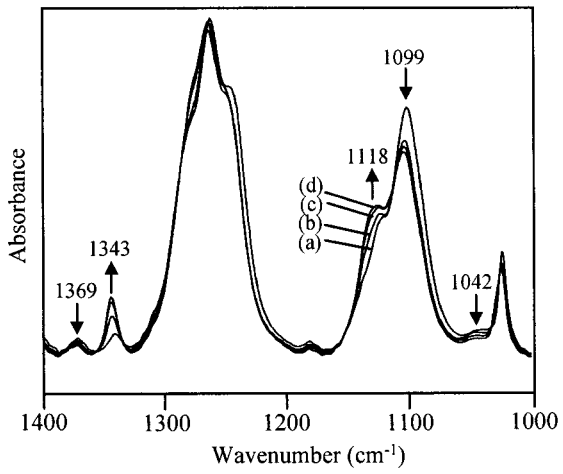

Figure 4. In situ FT-IR spectral change of PET on annealing at 210 °C: (a) 0, (b) 10, (c) 20, and (d) 60 min.

LPE was synthesized from an AB type monomer and a B_2 type core for the purpose of comparison with the HBP. Figure 7 illustrates the chemical structure of LPE, where the branching is perfectly suppressed and the backbone structure is very similar to that of the HBP. The relative crystallinity in the LPE/PET blends as a function of annealing time is shown in Figure 8. The effect of LPE on the reduction of the crystallinity of PET was less than that of HBP(OH). Figure 9 illustrates the carbonyl peaks of LPE/PET blends after 1 h annealing.

Table 2. Glass Transition Temperatures (T_g's) of HBPs, LPE, and Their Blends

sample	T_g (°C) real	T_g (°C) Fox equation
HBP(OH)	23	
HBP(Ac)	−5	
HBP(Bz)	34	
LPE	18	
HBP(OH)/PET = 20/80 wt %	74	66
HBP(Ac)/PET = 20/80 wt %	62	58
HBP(Bz)/PET = 20/80 wt %	69	69
LPE/PET = 20/80 wt %	68	66

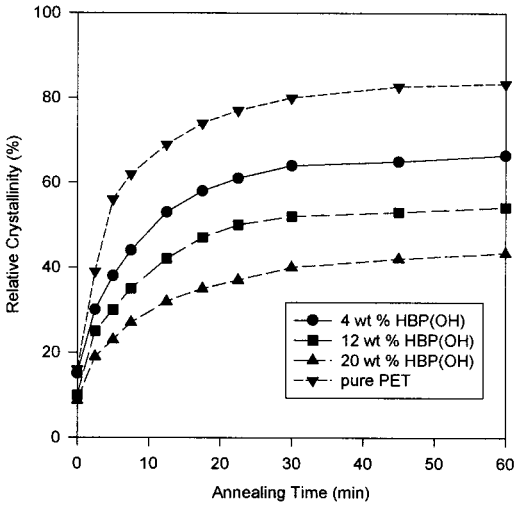

Figure 5. Relative crystallinity with increasing annealing time in HBP(OH)/PET blends.

Unlike the HBP(OH)/PET blends, the half-width of the C═O peaks in the LPE/PET blends was not increased. LPE could not form hydrogen bonds with PET as much as the HBP did. Therefore, the crystallization of PET in the LPE/PET blends was less suppressed than that in the HBP/PET blends.

Figure 10 presents the relative crystallinity of PET in HBP(Ac)/PET blends with increasing annealing time. The relative crystallinity was linearly reduced in proportion to the amount of HBP(Ac). The effect of HBP(Ac) on the reduction of the crystallinity of PET was less than that of HBP(OH) but similar to that of LPE. This can be explained by the fact that HBP(Ac) could not form hydrogen bonds with PET due to the absence of hydroxyl groups.

The relative crystallinity of PET in HBP(Bz)/PET blends with increasing annealing time is shown in Figure 11. Unlike HBP(OH) and HBP(Ac), HBP(Bz) increased rather than reduced the relative crystallinity

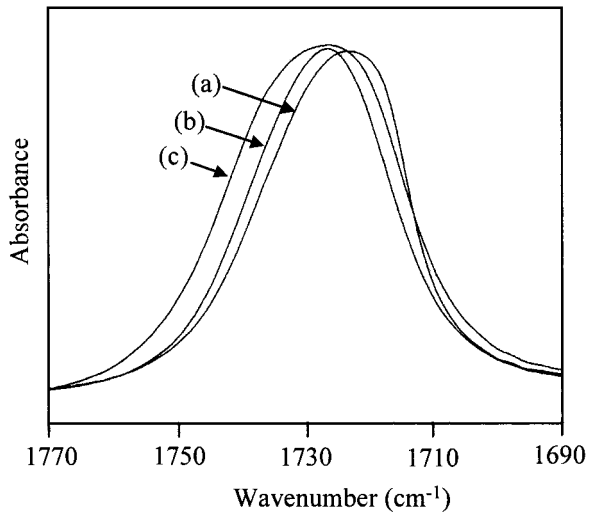

Figure 6. Carbonyl peaks of HBP(OH)/PET blends after 1 h annealing at 210 °C: (a) 4 wt % HBP(OH), (b) 12 wt % HBP-(OH), and (c) 20 wt % HBP(OH).

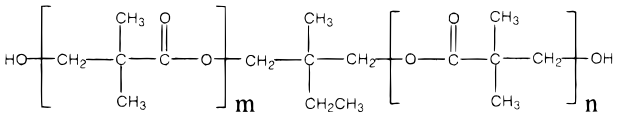

Figure 7. Chemical structure of linear polyester.

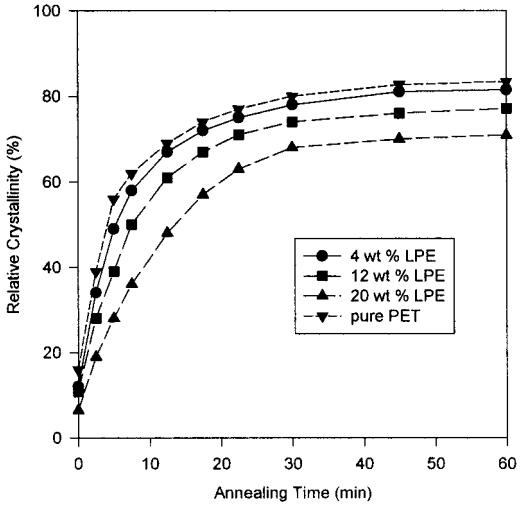

Figure 8. Relative crystallinity with increasing annealing time in LPE/PET blends.

in the blends. The crystallinity was increased until about 12 wt % HBP(Bz) with increasing the composition of HBP(Bz). Over the composition, the crystallinity was rather reduced with increasing the composition of HBP-(Bz). In the blend with 20 wt % HBP(Bz), the crystallinity became lower than that in pure PET. It seems that a small amount of HBP(Bz) can play the role of a nucleating agent during the crystallization of PET in HBP(Bz)/PET blends. The optimum concentration of HBP(Bz) as a nucleating agent was approximately 12 wt %.

Table 3 presents the melt crystallization temperature (T_{mc}) obtained from the dynamic DSC experiment. HBP-(OH) and HBP(Ac) decreased T_{mc}, whereas HBP(Bz) increased T_{mc} with the exception of 20 wt % HBP(Bz). The higher the value of T_{mc}, the higher the crystallization rate.[29] These results suggest that HBP(OH) and HBP(Ac) reduce the crystallization rate of PET with

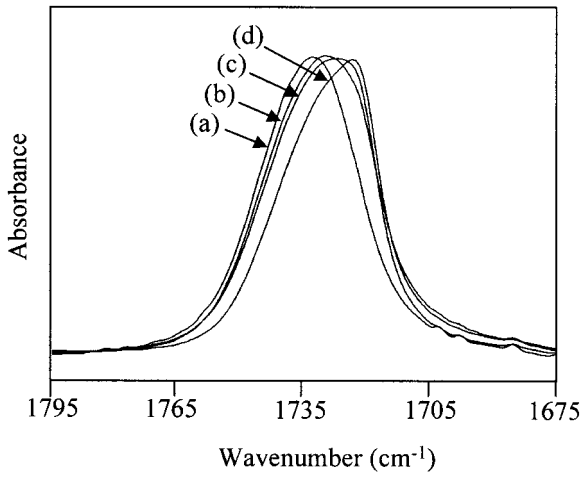

Figure 9. Carbonyl peaks of LPE/PET blends after 1 h annealing at 210 °C: (a) 20 wt % LPE, 0 min; (b) 20 wt % LPE, 1 h; (c) 12 wt % LPE, 1 h; and (d) 4 wt % LPE, 1 h.

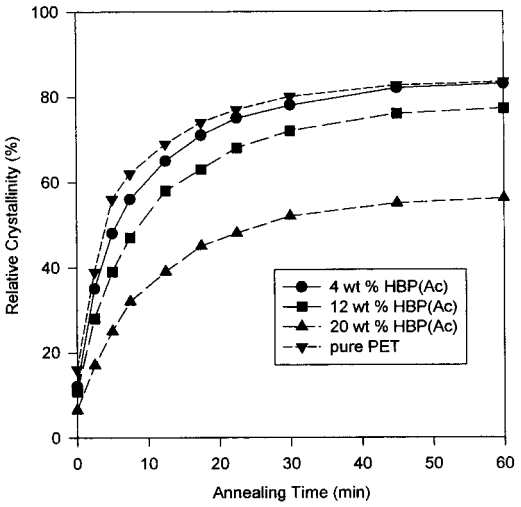

Figure 10. Relative crystallinity with increasing annealing time in HBP(Ac)/PET blends.

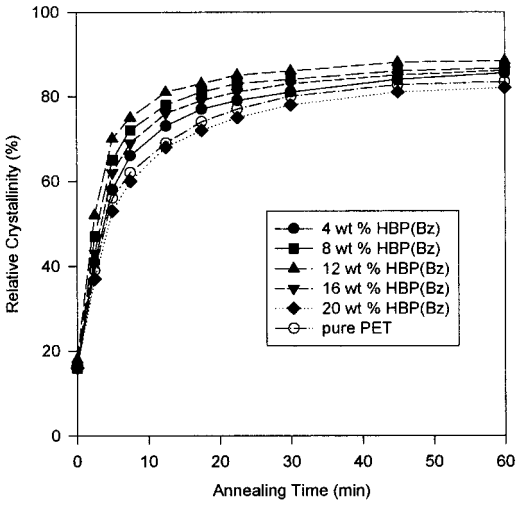

Figure 11. Relative crystallinity with increasing annealing time in HBP(Bz)/PET blends.

increasing composition, whereas HBP(Bz) increases the crystallization rate of PET. This means that HBP(Bz) acts as a nucleating agent. These results are consistent with those obtained from the in situ FT-IR experiment. It is believed that the terminal benzene rings of HBP-

Table 3. Melt Crystallization Temperatures (T_{mc}'s) of PET, HBP/PET, and LPE/PET Blends

sample	comp (wt %)	T_{mc} (°C)	sample	comp (wt %)	T_{mc} (°C)
PET	100	204	HBP(Bz)	4	207
HBP(OH)	4	202		8	210
	12	199		12	211
	20	196		16	207
HBP(Ac)	4	203		20	204
	12	202	LPE	4	203
	20	200		12	201
				20	199

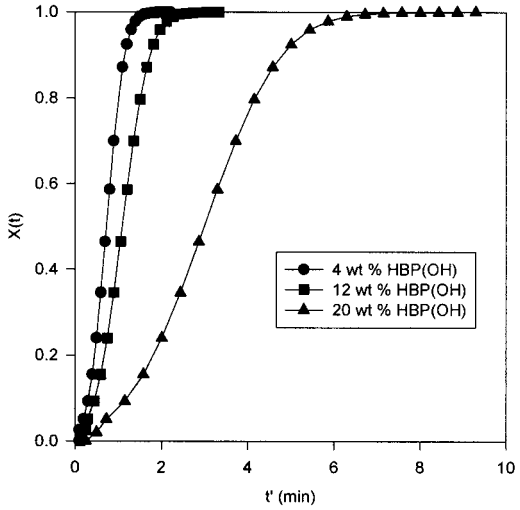

Figure 12. Crystallization isotherms of HBP(OH)/PET blends at T_c = 210 °C.

(Bz) increase the coplanarity of the benzene rings of PET and facilitate the trans form alignment of the ethylene glycol residue of PET. However, excess HBP(Bz) of over 20 wt % seems to act as a steric hindrance to the chain folding of PET.

Theoretical Consideration. Kinetic analysis can be carried out using the following Avrami equation:[30−32]

$$X(t) = 1 - \exp[-k(t - t_{start})^n] \quad (1)$$

where $X(t)$ is the fraction of the polymer crystallized at time t, k the overall kinetic constant, t is the time of the isothermal step measured from the achievement of the temperature control, t_{start} is the initial time of the crystallization process, which is determined from the subtraction of thermograms of sample and blank, and n is the Avrami exponent, which is related to the type of nucleation and to the geometry of the growing crystals. Figure 12 shows $X(t)$ as a function of time, $t' = t - t_{start}$, for HBP(OH)/PET blends. A remarkable reduction of the crystallization rate is observed with increasing composition of HBP(OH). Equation 1 can be expressed in the following form:

$$\log[-\ln\{1 - X(t)\}] = n \log t' + \log k \quad (2)$$

Plotting the first term versus log t', both k and n can be obtained from the slope and the intercept at log $t' = 0$, respectively. The rate coefficient can also be calculated from the half-life for the crystallization, $t_{0.5}$, through the following equation:

$$k' = \ln 2/t_{0.5}{}^n \quad (3)$$

Figure 13 exhibits the plotting of eq 2 for HBP(OH)/PET blends. The deviation from linear behavior, which is observed at high conversions, can be attributed to secondary crystallization phenomena, which take place inside a spherulite.

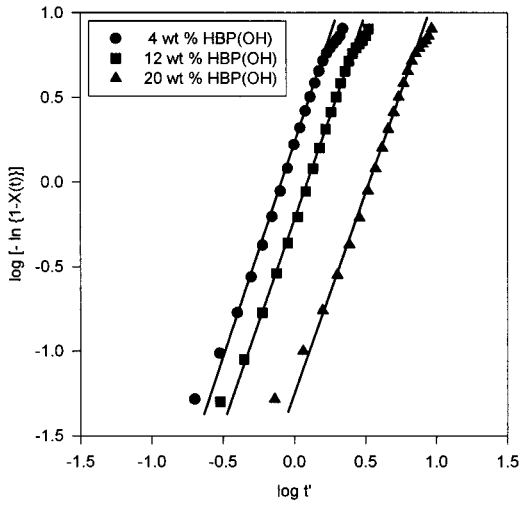

Figure 13. Avrami plots for HBP(OH)/PET blends at T_c = 210 °C.

Table 4. Relative Crystallinity, Heat of Fusion and Avrami Constants for PET, HBP/PET, and LPE/PET Blends

				Avrami constants	
sample	comp (wt %)	X(1 h)[a] (%)	ΔH_f[b] (J/g)	n[c]	k'[d] (min^{-n})
PET	100	83.4	64.5	2.8	1.725
HBP(OH)	4	66.5	54.7	2.5	1.250
	12	54.2	52.6	2.4	0.833
	20	43.4	44.8	2.3	0.033
HBP(Ac)	4	83.0	63.2	2.6	1.721
	12	77.2	59.2	2.9	1.510
	20	56.1	53.4	2.8	1.131
HBP(Bz)	4	85.5	64.9	2.7	1.730
	8	86.6	66.8	2.6	1.810
	12	88.4	68.4	2.5	2.189
	16	86.1	65.3	2.6	1.803
	20	82.3	62.2	2.6	1.610
LPE	4	81.5	61.5	2.7	1.718
	12	77.1	58.5	2.6	1.491
	20	70.9	56.8	2.6	1.289

[a] Relative crystallinity after 1 h annealing at 210 °C. [b] Heat of fusion in the dynamic DSC experiment. [c] Avrami exponent. [d] Rate coefficient obtained from the half-life for the crystallization.

Table 4 shows the relative crystallinity after 1 h annealing, Avrami constants (n, k'), and the heat of fusion for HBP/PET and LPE/PET blends. In all blends except the HBP(OH)/PET blends, the Avrami exponent, n, was about 3, which suggests instantaneous nucleation with spherical growth geometry. In the case of HBP(OH)/PET blends, n was about 2, which means instantaneous nucleation with disk growth geometry. The larger k', the higher the crystallization rate. The trend of the rate constants was very similar to that obtained from the FT-IR experiment. In the case of HBP(OH), the value of k' was greatly reduced with increasing composition of HBP(OH). Unlike HBP(OH) and HBP(Ac), HBP(Bz) increased k' more than that of pure PET with the exception of 20 wt % HBP(Bz). The maximum value of k' for HBP(Bz)/PET blends appeared at 12 wt % HBP(Bz), which was in accord with the results obtained by the FT-IR experiment. The heat of fusion reflects the crystallinity. The tendency of the heat of fusion also corresponded with that of the relative crystallinity obtained by the FT-IR experiment.

Rheological Measurement. Rheological measurement was performed to investigate the role of the HBPs

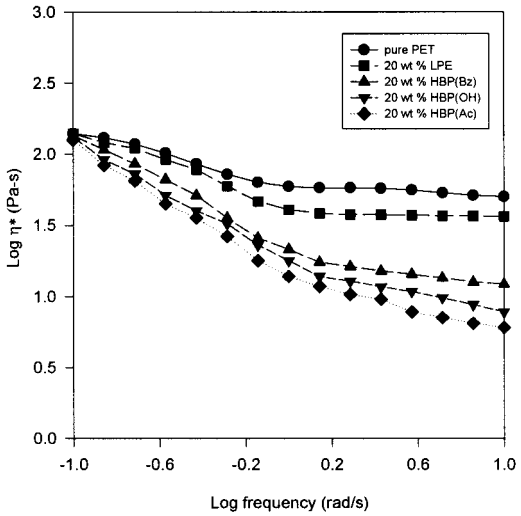

Figure 14. Complex viscosity as a function of frequency at T = 270 °C.

as processing aids in their blends. Figure 14 exhibits complex viscosity with increasing frequency. The viscosity drop in HBP/PET blends was larger than that in LPE/PET blends. These results show that HBPs can act as rheological modifiers in the blends. The trend of complex viscosity according to varying end groups was similar to that of glass transition temperatures (HBP(Bz) > HBP(OH) > HBP(Ac)). The order of T_g and complex viscosity for HBP(OH) and HBP(Bz) was opposite to that observed by Hult et al.[14,15] This is attributed to the fact that the generation of HBPs used in this study (the third generation) is lower than that in the experiments by Hult et al. (the fifth generation). Polar interaction of hydroxyl terminal groups in this system is less than that in their system. In addition, since the structures of HBPs used by them were closer to a globular structure, the steric hindrance derived from the rigid benzoate groups was more reduced, resulting in the descent of viscosity and T_g of HBP(Bz). That is the reason that the results of HBP(OH) and HBP(Bz) were switched in this study.

Conclusions

The crystallization behaviors of PET in HBP/PET blends were studied by in situ FT-IR spectroscopy and differential scanning calorimetry. The C═O stretching band of PET with increasing crystallinity was shifted to a lower wavenumber, which arose from the difference in coplanarity of the C═O with respect to the benzene ring. The increased dipole−dipole interaction could be a cause of the C═O band shift. Relative crystallinity could be obtained from the relative ratio of the areas of the two peaks corresponding to the gauche (1369 cm^{-1}) and trans CH_2 wagging vibration (1343 cm^{-1}).

The terminal groups and the composition of the HBPs had much influence on the crystallization behaviors of PET. A small amount of HBP(OH) could greatly reduce the relative crystallinity of PET through hydrogen bonds between the hydroxyl groups of HBP(OH) and the carbonyl groups of PET. The crystallization rate of PET could also be reduced by a small amount of HBP(OH). LPE synthesized from AB monomers could not decrease the relative crystallinity of PET as much as the HBP(OH) did. HBP(Ac) showed effects similar to those of LPE. It slightly reduced the crystallinity of PET in proportion to its amount in the blends. Unlike HBP(OH) and HBP(Ac), HBP(Bz) increased the crystallization rate of PET. The maximum of the crystallization rate appeared near 12 wt % HBP(Bz). Judging from the kinetic analysis of isothermal crystallization and the T_{mc}'s of dynamic crystallization, it is believed that HBP(Bz) plays the role of a nucleating agent in the blends. It was confirmed by rheological measurements that the HBPs acted as effective processing aids in the HBP/PET blends.

Acknowledgment. This work has been supported by Grant KOSEF 97-05-02-09-01-5 from the Korea Science and Engineering Foundation (KOSEF). The authors gratefully acknowledge the research support of KOSEF.

References and Notes

(1) The Polymer Society of Korea, Division of Polymer Synthesis, Spring meeting 1998, Seoul, Korea.
(2) American Chemical Society, Spring Meeting 1999, Anaheim, CA.
(3) The Polymer Society of Korea, Division of Hyperbranched Polymers and Dendrimers, Spring meeting 1999, Seoul, Korea.
(4) The Society of Polymer Science, Japan; *Kobunshi* **1998**, *47*.
(5) Fréchet, J. M. J.; Hawker, C. J.; Wooley, K. L. *J. Mater. Sci.: Pure Appl. Chem.* **1994**, *A31* (11), 1627.
(6) Denkewalter, R. G.; Kolc, J.; Lukasavage, W. J. U. S. Patent 4289872, 1981.
(7) Uhrich, K. E.; Hawker, C. J.; Fréchet, J. M. J. *Macromolecules* **1992**, *25*, 4583.
(8) Miller, T. M.; Neenan, T. X.; Kwock, E. W.; Stein, S. M. *J. Am. Chem. Soc.* **1993**, *115*, 356.
(9) Fréchet, J. M. J. *Science* **1994**, *263*, 1710.
(10) Hawker, C. J.; Farrington, P. J.; Mckay, M. E.; Wooley, K. L.; Fréchet, J. M. J. *J. Am. Chem. Soc.* **1995**, *117*, 4409.
(11) Mourey, T. H.; Turner, S. R.; Rubinstein, M.; Fréchet, J. M. J.; Hawker, C. J.; Wooley, K. L. *Macromolecules* **1992**, *25*, 2401.
(12) Kim, Y. M.; Kim, Y. G. *J. Ind. Eng. Chem.* **1999**, *5*, 74.
(13) Kim, Y. H.; Beckerbauer, R. *Macromolecules* **1994**, *27*, 1968.
(14) Malmström, E.; Hult, A.; Gedde, U. W. *Polymer* **1997**, *38*, 4873.
(15) Hult, A.; Johansson, M.; Malmström, E. *Macromol. Symp.* **1995**, *98*, 1159.
(16) Tomalia, D. A.; Naylor, A. M.; Goddard, W. A. *Angew. Chem., Int. Ed. Engl.* **1990**, *29*, 138.
(17) Boogh, L.; Pettersson, B.; Månson, J.-A. E. *Polymer* **1999**, *40*, 2249.
(18) Gopala, A.; Wu, H.; Xu, J.; Heiden, P. *J. Appl. Polym. Sci.* **1999**, *71*, 1809.
(19) Massa, D. J.; Shriner, K. A.; Turner, S. R.; Voit, B. I. *Macromolecules* **1995**, *28*, 3214.
(20) Carr, P. L.; Davies, G. R.; Feast, W. J.; Stainton, N. M.; Ward, I. M. Presented at the 35th IUPAC International Symposium in Akron, OH, July 11−15, 1994.
(21) Jang, J.; Oh, J. H. *Polymer* **1999**, *40*, 5985.
(22) Jang, J.; Sim, K. *Polymer* **1997**, *38*, 4043.
(23) Mencik, Z. *Chem. Prum.* **1967**, *17*, 78.
(24) Kimura, F.; Kimura, T.; Sugisaki, A.; Komatsu, M.; Sata, H.; Ito, E. *J. Polym. Sci., Part B: Polym. Phys.* **1997**, *35*, 2741.
(25) Miyake, A. *J. Polym. Sci.* **1959**, *38*, 479.
(26) Hannon, M. J.; Koenig, J. L. *J. Polym. Sci.* **1969**, *7*, 1085.
(27) Hwang, J. C.; Chen, C. C. *Polymer* **1997**, *38*, 4097.
(28) Shi, Y.; Jabarin, S. A. *Conf. Proc. ANTEC* **1998**, *2*, 2022.
(29) Kim, S. H.; Park, S. W.; Gil, E. S. *J. Appl. Polym. Sci.* **1998**, *67*, 1383.
(30) Avrami, M. *J. Chem. Phys.* **1939**, *7*, 1103.
(31) Avrami, M. *J. Chem. Phys.* **1940**, *8*, 212.
(32) Avrami, M. *J. Chem. Phys.* **1941**, *9*, 177.

MA991592C